J Ther Eng, Vol. 10, No. 6, pp. 1621−1631, November, 2024

Journal of Thermal Engineering
Web page info: https://jten.yildiz.edu.tr
DOI: 10.14744/thermal.0000871

Journal of Thermal Engineering

Research Article

Effect of porosity on thermal behaviour of sintered P/M iron material

T. K. KANDAVEL[1,*], J. VIGNESH, D. VIJAY[1]

[1]*School of Mechanical Engineering, SASTRA (Deemed to be University), Thanjavur, Tamil Nadu, 613 401, India*

ARTICLE INFO

Article history
Received: 05 March 2022
Revised: 21 June 2022
Accepted: 24 July 2022

Keywords:
Density; Iron; MATLAB; Powder Metallurgy; Sintering; Thermal Conductivity

ABSTRACT

Iron components processed through Powder Metallurgy (P/M) route have complex material characteristics due to the presence of pores. The present research work attempts to investigate the influence of porosity on the thermal conductivity of the sintered iron specimens. Green iron compacts of various densities were obtained by applying various compaction pressures. An electric muffle furnace with a capacity of 3.5kW was used for sintering the green compacts. The specimens of the same density were utilized to conduct thermal conductivity experiments. The Design Expert (DE) software has been used to design and conduct the thermal conductivity experiment on specimens. The variations of heat flow through the preforms were studied using ANSYS. Using MATLAB, a similar kind of study was also carried out, and the results were compared. The test results reveal that the thermal conductivity of the P/M iron increases with a decrease in porosity or increase in density.

Cite this article as: Kandavel TK, Vignesh J, Vijay D. Effect of porosity on thermal behaviour of sintered P/M iron material. J Ther Eng 2024;10(5):1621−1631.

INTRODUCTION

P/M iron components are gradually replacing the conventional solid components in various industrial sectors like structural, machinery industries, civil construction, hoisting equipment, etc., due to their excellent metallurgical, mechanical, and thermal properties. Though the P/M iron material has equivalent mechanical strength to wrought material, the pores in the material adversely affect the thermal behaviour of the material. The relative motion of the components generates heat, and the components must be able to dissipate the generated heat to the greater extent in order to retain the normal working condition in the actual applications. The present work aims to investigate the influence of porosity on thermal conductivity of the sintered iron specimen. The generalized correlations using DE and MATLAB software have also been developed to evaluate the thermal conductivity of P/M iron at different input parameters such as heat flux and density.

Vincent et al. [1] have investigated the influence of porosity on the thermal conductivity of copper preforms processed through the P/M route and reported that the thermal conductivity of the material decreases with increase in porosity. The infiltration pressure of the porous Al-12 wt. % Si/SiC composites invariably increases the thermal conductivity due to an inherent reduction in porosity [2]. Influence of pore size on thermal conductivity of porous wicks analyzed by Jiyuan et al. [3] has reported that the smaller pore sizes of material invariably lower the thermal conductivity of the material. Pia and Sanna [4] have investigated the

*Corresponding author.
*E-mail address: tkkandavel02@mech.sastra.edu

This paper was recommended for publication in revised form by Editor-in-Chief Ahmet Selim Dalkılıç

Published by Yıldız Technical University Press, İstanbul, Turkey

dependency of pore size on thermal conductivity through intermingled fractal units' technique and it was observed that for the same volume fraction of voids, the thermal conductivity is found to decrease with a reduction in the size of pores. The cooling rate of P/M steels is getting reduced with an increase in porosity level and subsequently a decrease in the material's hardness [5].

Daninnger et al. [6] have studied the effect of porosity variations on thermal expansion and thermal heat capacity of sintered steels and reported that the variation in porosity is found to have less effect on specific heat capacity of the material and the alloy content and the temperature at which the P/M steel is processed have some effects on specific heat capacity. It has been investigated and reported that the highly densified steel specimens are observed to have high thermal conductivity [7]. Gojic et al. [8] have investigated the hardness and microstructure of the steel, and it was found that the hardness has been increased by 200HV when the bainitic structure is transformed into the martensitic microstructure. Popovska et al. [9] have investigated the properties of porous silicon carbide and concluded that the high bridge density in the fiber network favours the thermal conductivity. The thermal conductivity of sintered metal powder compacts is found to have a lower thermal conductivity than stainless steel, copper, and bronze, the solid materials [10].

The investigation carried out by Tatar and Demir [11] on the thermal conductivity and microstructure of P/M Al_2O_3 particulate reinforced aluminium composites (Al/Al_2O_3-MMC) has concluded that the thermal conductivity of porous alumina could be enhanced by adding more amount of alumina powder. Zivcova et al. [12] have investigated the thermal conductivity of porous alumina ceramics prepared using starch as a pore-forming agent, and found that the pore size plays a vital role in the thermal conductivity of the material and it increases with a decrease in size of the pore. Kurt and Ates [13] have studied the effect of thermal conductivity on P/M processed materials and found that the compacting pressure plays an important role in the green density of P/M materials; increasing sintering temperature increases the green density of P/M materials. They have also reported that the thermal conductivity of the P/M steel samples increases with decreasing porosity ratio. Matsuo [14] has studied the effect of porosity on the thermal conductivity of nuclear graphite and concluded that the percentage change in thermal conductivity is approximately linear with the increase in open porosity. Ondracek and Schulz [15] have observed the porosity dependency on thermal conductivity of nuclear fuel (uranium di oxide) and have proposed an equation to calculate the thermal conductivity from the orientation of the pores orientation, such as shape and size. It is reported by the researchers that the thermal conductivity of crushed salt decreases with increasing porosity and temperature, and they have also reported in their results that the thermal diffusivity and specific heat of the substance have less dependence on the porosity [16]. Non-uniform pore size distributions have led to the reduced thermal conductivity of phase change materials [17]. The inclusion of porosity in a hydrocarbon reservoir in an Enhanced Oil Recovery (EOR) technique was found to increase the heat transfer to the fluids stored in it [18]. The increment of porosity was found to decrease the thermal conductivity of dry soil [19]. It was reported by the author in his research work that the hydrated fluid flow over the porous plate has a significant effect on the velocity, pressure, displacement, and stress, and on the other hand, it has less effect on the temperature [20]. Kandavel and Dhasarathy [21] have investigated the influence of sintering temperature on thermal behaviour of Cu-added iron materials. They have reported that the P/M component sintered at higher temperature possesses high thermal conductivity and at the same time, it increases the hardness of the component also.

Thermal properties of P/M material depends on various physical characteristics. Though, research work is going on in this field, researchers found difficult to arrive one generalized modeling as a whole for the P/M material. Unlike solid material, the behaviour of P/M material is a complex phenomenon. It has a special character of varying density and hardness, when it is subjected to any load. It is difficult to ascertain any common properties due to complexity. As a whole, it is necessary to identify the research gap and carryout the work in this field. P/M material never reaches 100% density, even it is subjected to high level compaction. Particularly, in porous (P/M) material the porosity plays a significant role in determining the thermal characteristics. The porosity level is determined by the way of making the component.

The present research work aims to study the influence of porosity on thermal behaviour of P/M iron components. Components of varying porosity level are achieved by varying the compaction pressure. Generalized correlations are established to find the thermal conductivities for the specimens of different porosity. By applying any input parameters such as heat flux and density of the material. One could be able to get the thermal conductivity of the specimen without any analytical calculations.

SYSTEM DESCRIPTION

The pure Iron powder was accurately weighed to the required quantity using 4 Decimal accuracy Shimadzu digital balance (made in Japan). The powder is compacted to the various densities by applying suitable compaction pressure on Universal Testing Machine (UTM, capacity 1000kN) using suitable cylindrical die-punch set with graphite as a lubricant. The green compacts of size Ø50×7mm with various percentages of theoretical densities such as 69%, 78%, and 86% were obtained by applying compaction loads 250, 350, and 500kN, respectively, during compaction. A specially made ceramic coating had been applied on the exposed surfaces of the green compacts to

prevent oxidation during the sintering process. Well-dried-coated green compacts were sintered in argon purged 3.5kW Muffle furnace (capacity 1100°C) at a temperature of 1050 ±10°C for a period of 30 minutes. The sintered specimens were then polished in belt emery to remove the oxides from the surface. The density of each specimen was found using the Archimedes principle, and hardness for the same specimen was identified using a Rock Well hardness tester. An indigenously fabricated fixture was used to conduct the thermal conductivity tests on the sintered iron specimens with different percentage theoretical densities. The sintered specimens of the same density were placed on either side of the heater coil, and K-type thermocouples were placed at four points on either side of the specimen, i.e., in between the heater coil and the specimen and outer side of the specimen to observe the heater coil temperature and on the other side of the specimen corresponding to the amount of heat conducted through the specimen.

The experimental setup is illustrated in Figure 1. Insulating materials (glass wool pockets) were packed around the heater coil specimens' setup to avoid any form of heat loss during the experiment. The entire set up was placed inside an enclosure to eliminate the atmospheric interference. The thermal conductivity experiment was conducted at various set voltages such as 50, 60, 70, 80, and 90V by controlling dimmerstat. The temperatures of the thermocouples placed at the various positions were observed from the digital display connected with the experimental setup. All the temperature readings were noted only after the attainment of steady-state conditions. The thermal conductivity of each voltage setting for various densities of the sintered iron specimens was calculated as per Fourier's law of heat conduction.

The experimental results were further analyzed using DE and MATLAB software to predict the thermal conductivity at any input parameters. The results of both the software were compared tor assess the level of agreement with the experimental results. A generalized correlation has been established to find the thermal conductivity of various densities of iron specimens relating to the theoretical density and heat flux using DE software. The experimental results were fed to ANSYS APDL software to study the variation of temperature distribution across the specimen surface of various densities of the sintered iron specimens. The microstructures of the various densities of sintered iron specimens have been captured using 1000X optical microscope (Make: Japan, KYOWA, ME-LUX2) with image analyzer and have been corroborated with the experimental results.

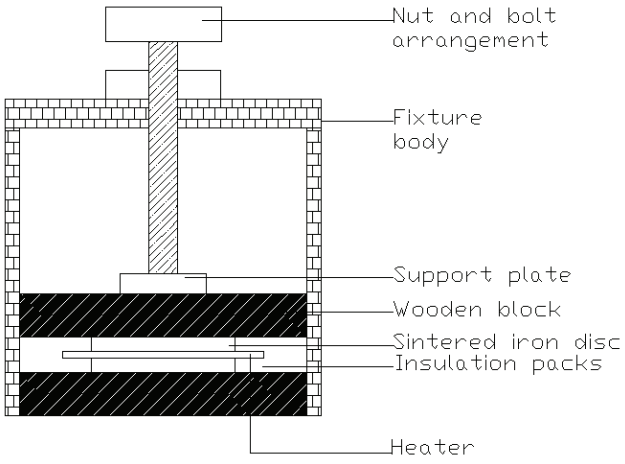

Figure 1. Experimental setup.

RESULTS AND DISCUSSION

Solid iron components possess higher thermal conductivity compared to P/M iron components [10]. Though the P/M components are inferior in some quality, they are competitive in strength compared with the conventional solid material. In the present work, the thermal behaviour of sintered iron components has been investigated with the variation of density/hardness of iron specimens by conducting thermal conductivity tests.

Influence of Porosity on Hardness and Thermal Conductivity of the Sintered Iron Preforms

A set of the sintered iron preforms of equal density is considered for the thermal conductivity test. The specimens of equal density are placed as per the experimental arrangement shown in Figure 1. Required numbers of thermo-couple are provided at suitable positions to monitor the temperatures of the specimen on either side. The temperatures on either side of the specimen were noted, and the average value temperatures and other values such as the heat flux and the thermal conductivity of the sintered preforms were also calculated using the Fouriers' Law of Conduction correlation (Eq. 1).

$$k_s = \frac{q.t}{T1 - T2} \tag{1}$$

'q' represents heat flux in $\frac{W}{m^2}$ since $q = \frac{Q}{A} = \frac{V*I*(p.f)}{\frac{\mu*(d^2)}{4}}$

where,
V= Voltage (V)
I = Current (A)
p.f = Power factor (%) = 0.86
d = Diameter (mm)
k_s = Thermal conductivity if the specimen in $\frac{W}{m°C}$
T1 = Specimen temperature at coil side in °C
T2 = Specimen temperature at opposite side in °C

Based on the experimental tests, the values of hardness and thermal conductivity of sintered iron preforms at various densities are illustrated in Table 1. The bar chart shown in Figure 2 illustrates the hardness value of the sintered iron specimens at various densities. It is clearly evident from the

figure that the specimen processed with high compaction pressure is found to have higher hardness due to an increase in the density of green compacts [5]. Higher compaction pressure makes the green compacts with less number of smaller size pores compared with the preforms made with lower compaction pressure. The minimum hardness value of 68.6 HRB is obtained for 69% theoretical density, and the highest hardness of 84 HRB is obtained for 86% theoretical density of the iron specimen.

Though the thermal conductivity of heat through the metal is a natural phenomenon, the thermal conductivity of P/M metal depends on number of parameters such as porosity, density, size, and shape of elemental powders, alloying elements, etc. The present investigation is focussed on the influence of porosity/density on the thermal conductivity of the sintered iron preforms. The various levels of porosity/density of the specimens are achieved during the compaction by applying the required level of compaction pressure. However, some of the post sintering operations like upsetting, forging, etc., could also be used for varying porosity or density of the sintered specimen. Increasing the density of the P/M part is observed to improve the thermal conductivity behaviour of the P/M material [7]. The maximum thermal conductivity (18.91W/m°C) of the sintered iron is exhibited by the 86% theoretical density of the iron preform at the maximum heat flux input (Table 1). This thermal conductivity value for the 86% density of the material is 35% higher than that of 69% density material and 23% greater than that of 78% density material. Pores present in the P/M materials contribute to the heat loss during the heat conduction, which in turn leads to lower the thermal conductivity of P/M material. Decreasing the pores or otherwise increasing the density is found to increase the thermal conductivity of the sintered P/M iron specimens [7].

Thermal Behaviour Modeling of the Sintered Iron Preforms

The thermal behaviour modeling for various densities of the sintered iron material has been generated using DE and MATLAB software. The 3D modeling generated by the

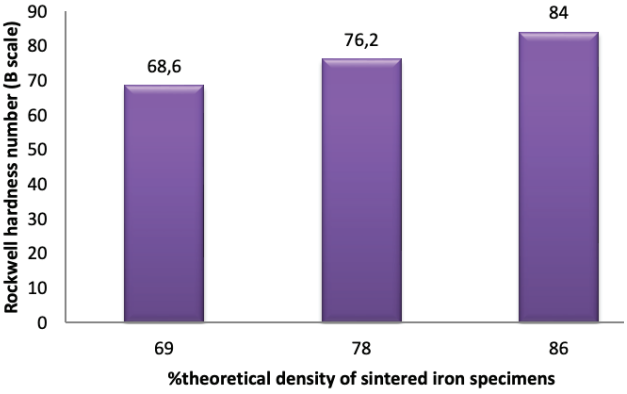

Figure 2. Bar chart of hardness for various densities of sintered iron specimens.

Table 1. Comparison of thermal conductivity of sintered iron preforms using Design Expert and MATLAB software

%theoretical density of iron preforms	Rockwell hardness (HRB)	Experimental input and output parameters							
		Voltage (V)	Current (A)	Heat flux (W/m²)	Thermal Conductivity (W/m °C)				
					Experimental Value	ANOVA Value	Percentage Error	MATLAB Value	Percentage Error
69	68.6	50	0.160	1401.018	02.50	02.48	-00.80	02.75	10.19
		60	0.194	2123.418	03.64	03.28	-09.89	03.56	-02.18
		70	0.250	3283.636	06.06	05.48	-09.57	05.77	-04.69
		80	0.280	4290.618	07.80	08.31	06.53	08.61	10.50
		90	0.300	5253.818	12.20	11.81	-03.19	12.13	-00.49
78	76.2	50	0.160	1401.018	03.87	03.45	-10.85	03.79	-01.82
		60	0.194	2123.418	05.00	04.63	-07.40	04.98	-00.22
		70	0.250	3283.636	07.88	07.45	-05.45	07.82	-00.75
		80	0.280	4290.618	11.88	10.81	-09.00	11.20	-05.72
		90	0.300	5253.818	14.54	14.83	01.99	15.23	04.76
86	84	50	0.160	1401.018	05.21	04.65	-10.74	05.07	-02.58
		60	0.194	2123.418	06.90	06.17	-10.47	06.60	-04.26
		70	0.250	3283.636	09.12	09.54	04.60	09.98	09.50
		80	0.280	4290.618	14.71	13.38	-09.04	13.81	-06.10
		90	0.300	5253.818	18.91	17.85	-05.60	18.32	-03.06

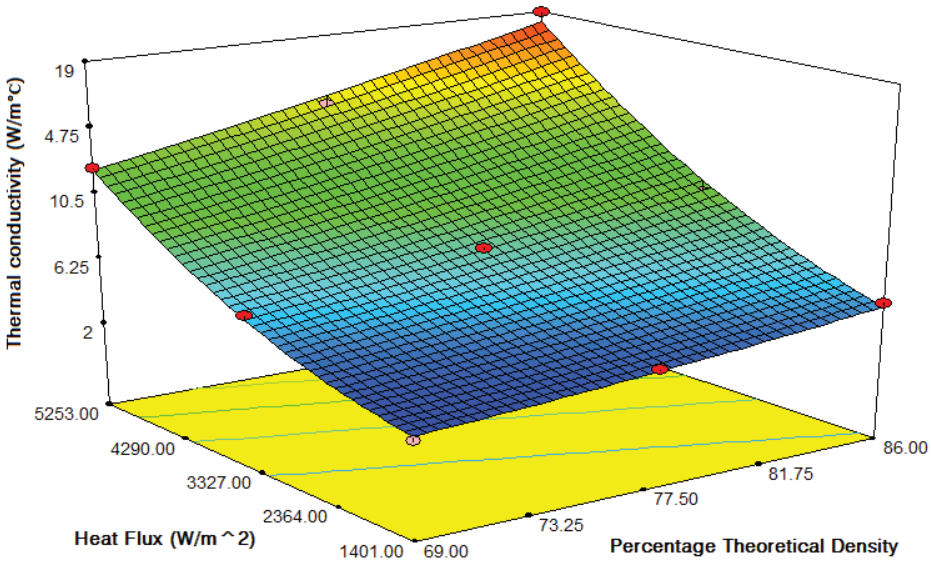

(a)

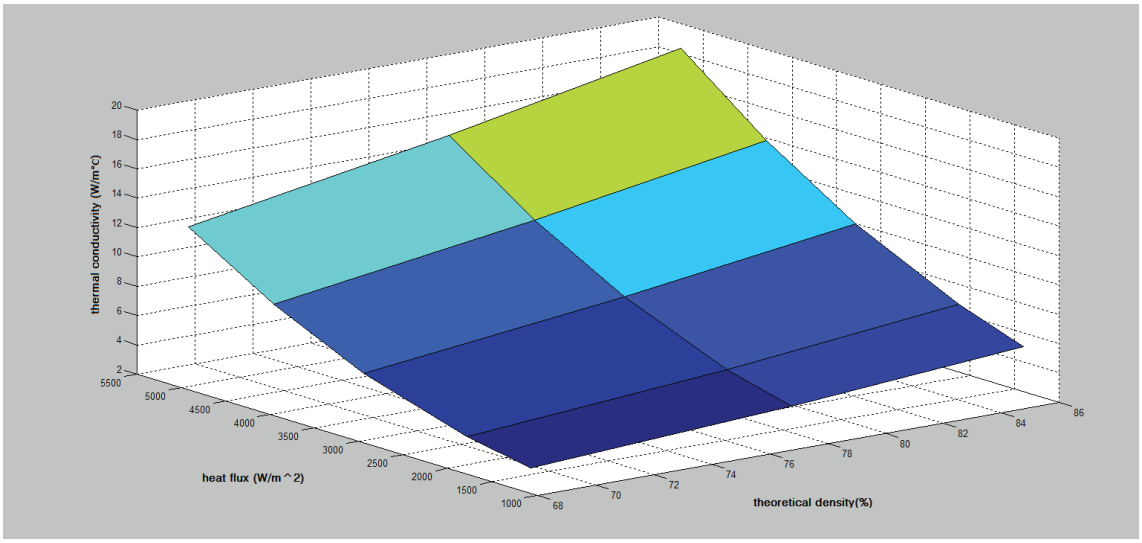

(b)

Figure 3. 3D models for thermal behaviour of sintered iron preforms, a) Design Expert, and b) MATLAB softwares.

software is illustrated in Figure 3. The 3D models developed by this software are useful for analyzing the thermal conductivity at any given input parameters. The images in Figure 3a and 3b are the 3D models developed by the DE and MATLAB software, respectively. The colour variations towards the increasing input parameters show the level of increased thermal conductivity of the material. It is observed from the 3D images of both the software that the thermal conductivity of the sintered iron is increasing linearly with respect to density of the material and the amount of heat supplied [14]. The images developed by the software are found to be similar in appearance.

A generalized correlation has been generated [15] from the regression analysis by DE software to find the thermal conductivity of various densities of the sintered iron specimens and the generalized equation is given in Eq. 2.

$$k = (13.91364) - (0.34260\ X) - (4.44915\times10^{-3}\ Y) + (5.90984\times10^{-5}XY) + (2.55674\times10^{-3}\ X^2) + (4.21953\times10^{-7}\ Y^2) \quad (2)$$

where, k = Thermal conductivity in $\frac{W}{m°C}$

X = Theoretical density in %

Y = Heat flux in $\frac{W}{m^2}$

Using the generalized correlation given in Eq. 2, the thermal conductivity of the sintered iron specimens could be arrived at by mere substituting the input parameters such as theoretical percentage density and heat flux [15].

The regressive quadratic equations generated using the DE software were used to get the numbers of response parameter and were used in MATLAB. The equations were subjected to computation using the subsequent programming steps. The entire results which were obtained using the computation were arranged into an array. Using the surf command the values stored in the array were plotted in the 3D surface graph.

Figure 4 shows the images of heat flow distribution across the specimen generated for the various densities of the sintered iron preforms at the lowest and highest heat supplied by ANSYS-APDL software. The input parameters for determining the thermal conductivity of the sintered iron specimens are fed in the software. The software has generated the image illustrating the distribution of heat flow across the specimen based on the density and heat flux. The variation of colours and their intensity describe the distribution of heat and the level of heat conduction in the specimen. As the specimens are porous, the colour variations and their intensity are found to be scattered across the specimen. Images are shown in Figure 4a illustrate the heat flow pattern through the 69% theoretical density of the sintered iron preforms. The heat conductivity at the lowest density of specimen is found to be lower compared to higher density specimens [1,2, 16]. This is due to the fact that lowest density of specimen has higher porosity. The heat distribution over the region is observed as random or more scattered due to the presence of high degree of pores in the specimen. The voids in the specimen are found to scatter the heat and reduce the thermal conductivity of the P/M material. The densified specimen is observed to exhibit higher thermal conductivity due to the lesser number and smaller pores [3, 4]. Figure 4b and 4c show the thermal conductivity of densified specimens. The distribution of colours and their intensities are found to be uniform for 78% of densified specimens and more uniform for the 86% of densified specimens, as shown in Figure 4b and 4c. The maximum densified specimen (86%) at the maximum heat flux is found to have the highest thermal conductivity (18.91 W/m °C) in the entire experimental range. The ANSYS image is also observed to prove this phenomenon by showing the uniform distribution of yellow colour with almost same intensity over the entire region of the specimen surface for the highest density and at the maximum heat flux.

Comparison of Design Expert and MATLAB Values with Experimental Results

Comparative charts have been made in order to investigate the closeness of software values such as ANOVA and MATLAB with the experimental results at various input voltage for three different percentage theoretical density specimens. The cumulative comparison chart is shown in Figure 5a-c.

Figure 5a shows the comparative plot for thermal conductivity of 69% theoretical density specimen. The maximum experimental value (12.20W/m °C) is exhibited at the highest input power (90V). The corresponding ANOVA and MATLAB values are 11.81 and 12.13 W/m °C respectively. The percentage error found for the MATLAB at this value is -00.59 and for ANOVA, it is -0.3.19. The values are indicating the closeness of software's value with the experimental. Similarly for 78% theoretical density specimen, the comparative plot is made and shown in Figure 5b. The pores available in the specimen are lesser than the 69% density specimen. One can expect higher thermal conductivity at the same higher input power (90V) from the specimen. The highest experimental thermal conductivity exhibited at the highest input power is 14.54W/m °C. The corresponding values of ANOVA and MATLAB are 14.83 and 15.23W/m °C respectively. The percentage errors of these values with the experimental value are 01.99 and 4.76. The lower error values are indicating the closeness of these values with the experimental value. The cumulative thermal conductivity of both the experimental and software plot for 86% density specimen is depicted in Figure 5c. Naturally, the thermal conductivity of the specimen is found to be higher due to pores reduction. The specimen is exhibiting the highest thermal conductivity (18.91W/m °C) at the highest input power among the other two density specimens. Using ANOVA and MATLAB, the thermal conductivity of the specimen are 17.85 and 18.32W/m °C. The corresponding error values calculated are -05.60 and -03.06 respectively. Though, the error values are lower in all the cases irrespective of input power and specimen densities, seem to be a perfect alignment of software's value with the experimental value. The following observations are made from the plots that i) the trend is same for all the thermal conductivity values, ii) the line of software value merge with the experimental value, indicating the closeness of value. At the outset, the software could be used to develop thermal behaviour modeling for any P/M materials.

Using the mathematical models generated by regression analysis (DE) and MATLAB software, the thermal conductivity of the specimen for various densities and heat inputs has been calculated. The evaluated conductivity values from this software are summarized in Table 1. The deviation from the experimental values is given as a percentage error in Table 1. The error values obtained from the mathematical models generated by regression analysis (DE) and MATLAB software are compared and illustrated in Figure 6. It can be seen from Figure 6 that the deviations are poised equally on either side of the nominal value (experimental value) for the values obtained from the mathematical models. The same kind of wavy trend is also observed in the plots. In both cases, the percentage error has not been exceeded 11%. It shows that the values obtained from two different modeling have good agreement with the experimental values. It may be concluded that the DE software and MATLAB could be used for predicting and analyzing the thermal behaviour of porous P/M materials.

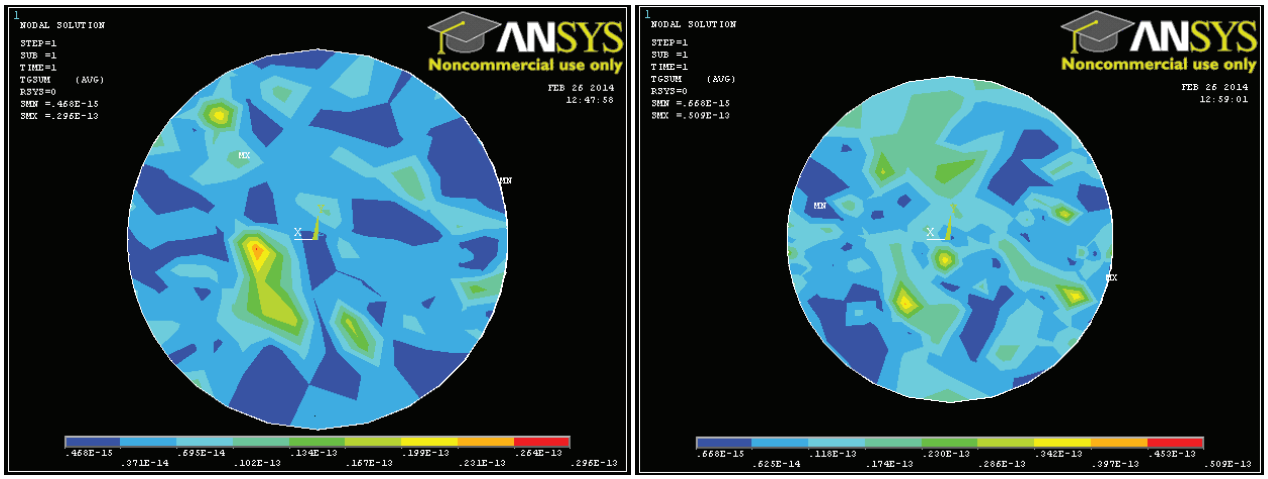

(i) 50V (ii) 90V

(a)

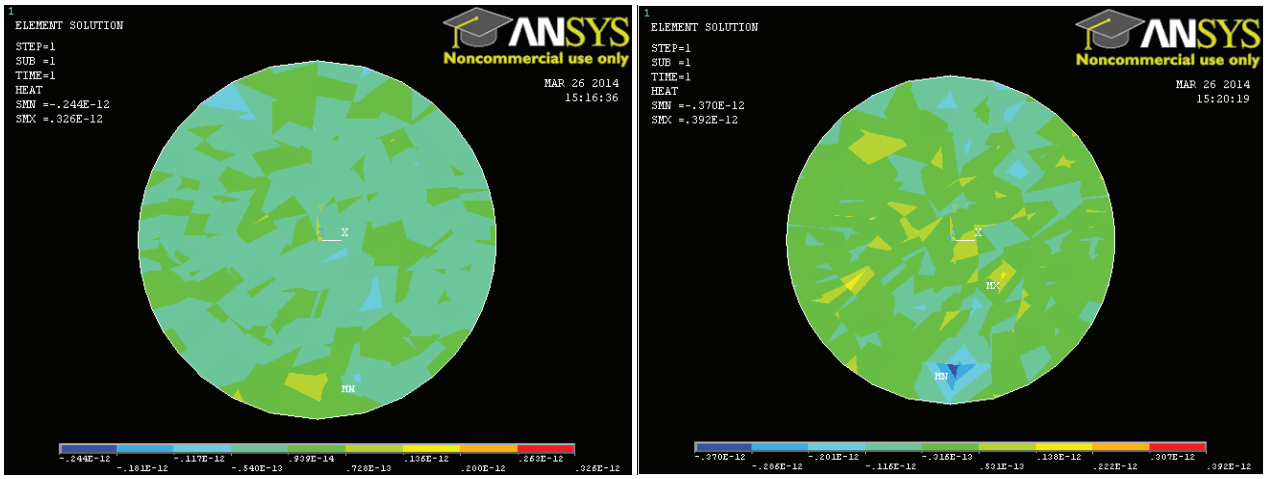

(i) 50V (ii) 90V

(b)

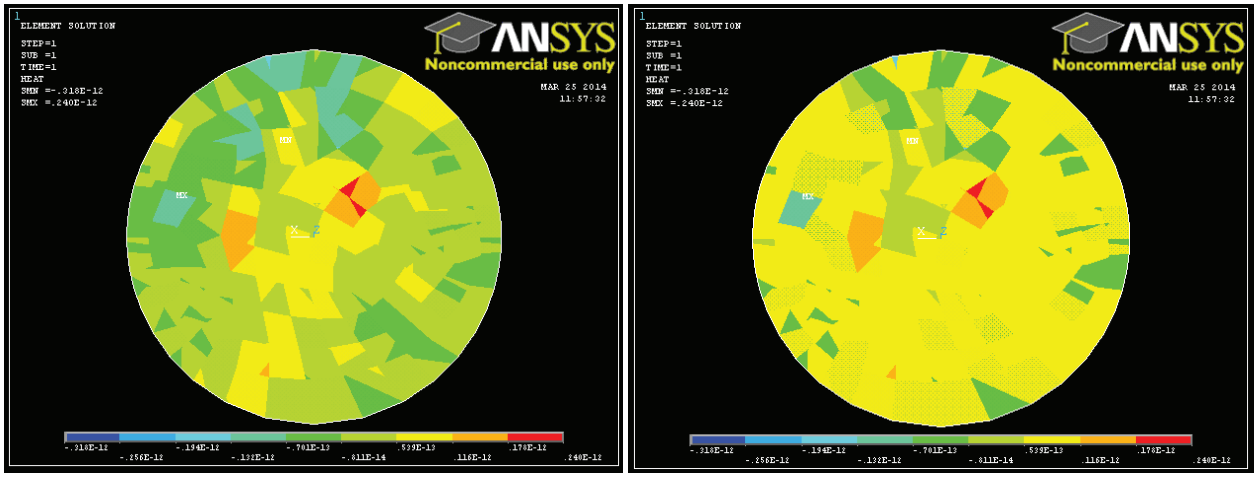

(i) 50V (ii) 90V

(c)

Figure 4. ANSYS images of thermal flow through the sintered iron specimens of various % theoretical densities at 50V and 90V power supply, a) 69%, b) 78%, c) 86%.

Analysis of Microstructure and Pore Distribution of the Sintered Iron Preforms

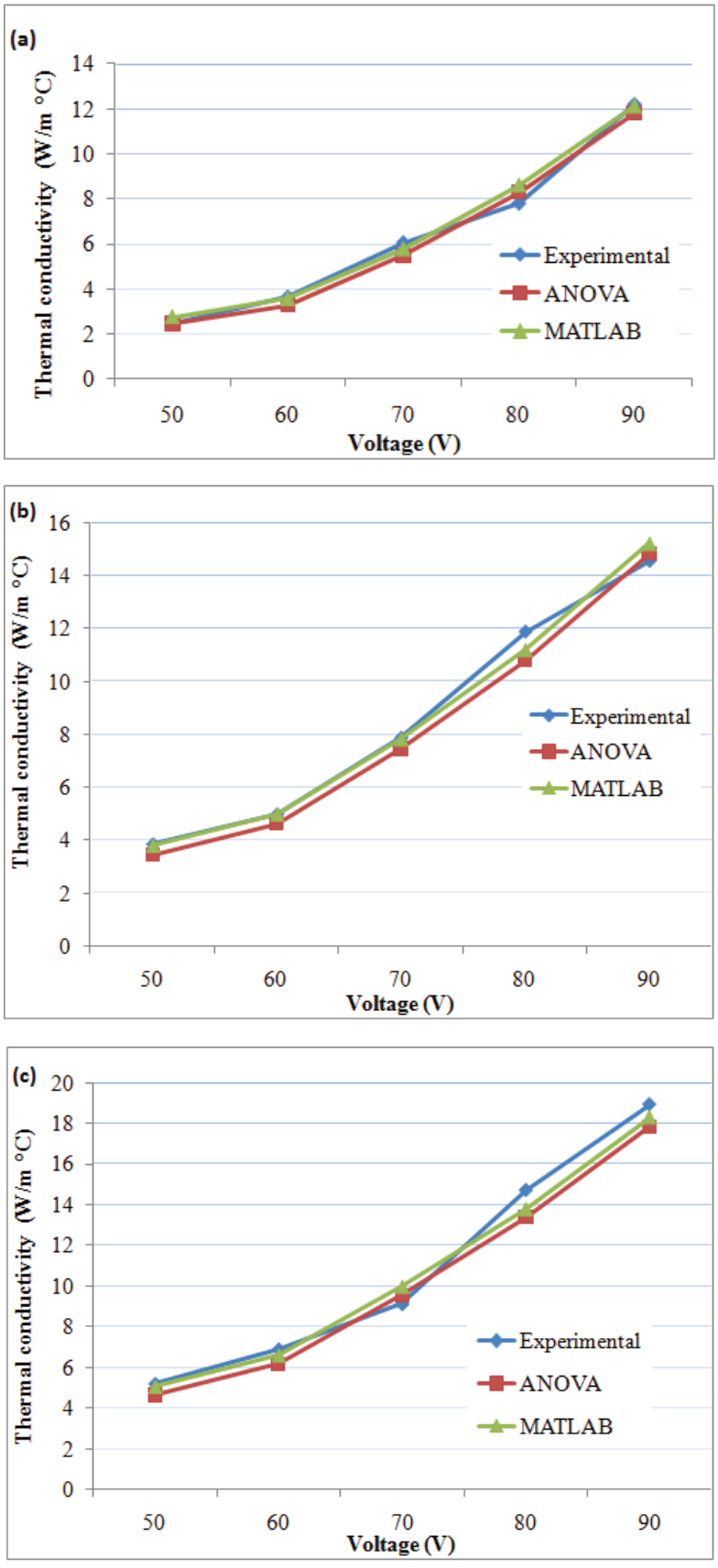

Figure 5. Comparison of experimental thermal conductivty value with ANOVA and MATLAB for different percentage theoretical density specimens, (a) 69%, (b) 78%, (c) 86%.

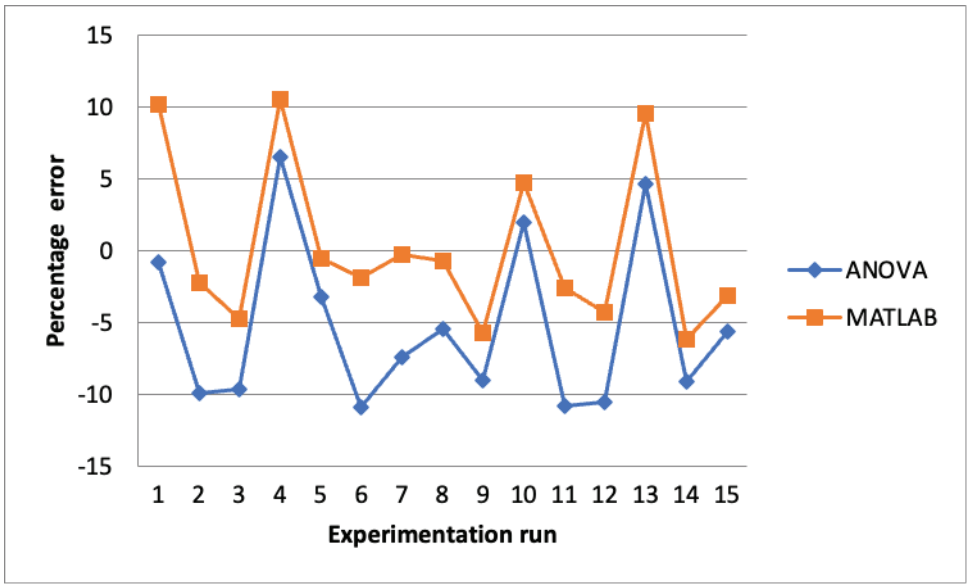

Figure 6. Comparison of the percentage errors obtained from the models generated by regression analysis (DE) and MATLAB software.

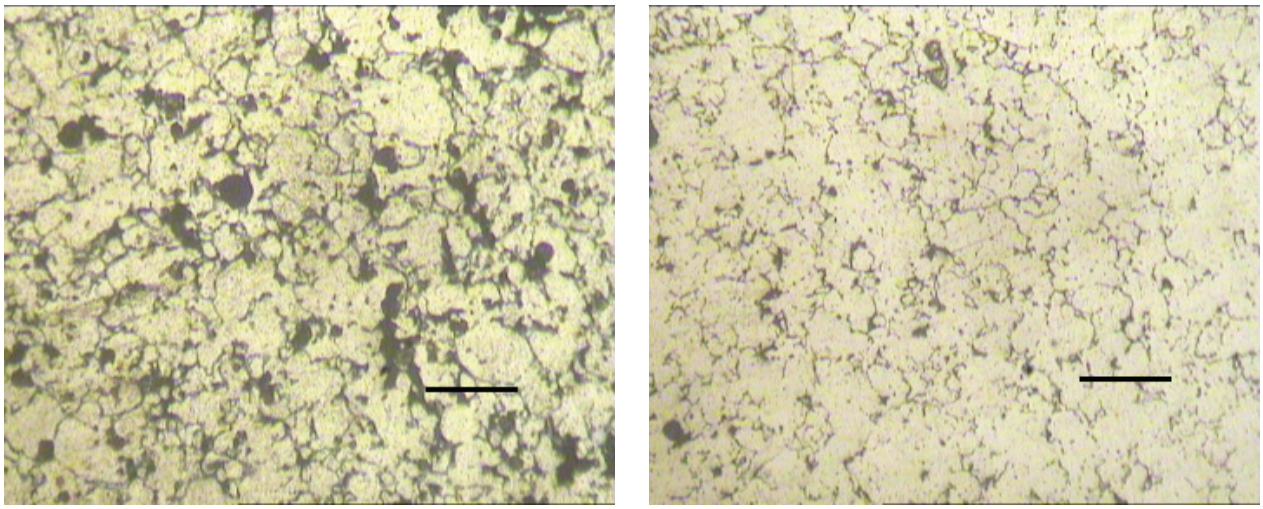

(a) **(b)**

Figure 7. Microstructures of various % theoretical densities of the sintered iron preforms, a) 69% and b) 86%.

Figure 7 shows the microstructures of the sintered iron preforms prepared with various densities. Figure 7a and 7b show the morphology of the 69% and 86% densified sintered iron preforms, respectively. The ferritic microstructure is found in both cases of the iron preforms. Figure 7a shows the surface morphology of the 69% theoretical percentage of iron specimen. It is observed from the images that the grain sizes and pore sizes of the lower density preforms are found to be bigger compared to the higher density preforms. Numbers of pores are found to be more and also bigger for the lower (69%) densified specimen. The pores are non-uniform in size and randomly poised in the ferritic matrix. The non-uniform size of pores has led to reducing the thermal conductivity of the specimen [17]. The percentage of pores present in the ferritic matrix is about 16%, and the corresponding average pore size is 0.0576 μm^2. Figure 7b shows the micro optical image of the maximum densified iron specimen (86%). Little elongated grain structure is observed for the well-densified preforms. Uniformly distributed pores are seen in the image. The percentage of pores occupied in the ferritic matrix is about 7%, and the corresponding average pore size is about 0.0288

μm^2. From the images of microstructure, it may be concluded that the grain size, number of pores, and pore size determine the thermal behaviour of P/M materials [3, 4]. Grains of smaller size with less number of pores are found to conduct more heat than the grains of bigger size. The P/M components processed with higher compaction pressure or higher density are found to exhibit higher thermal conductivity [7].

CONCLUSION

Based on the experimental work carried out on the sintered iron preforms of various percentage theoretical densities to investigate the influence of porosity on thermal characteristics, the following conclusions could be drawn:

- The thermal conductivity of the sintered iron increases with a decrease in porosity of the material.
- Increasing the density of sintered P/M iron material improves the hardness and thermal behaviour.
- The sintered iron's thermal conductivity depends on the specimen's heat flux.
- The higher percentage (16%) of pores, and pore size (0.0576 μm^2) is found in the lower density (69%) P/M iron specimen.
- The lower percentage of pores (7%) and pore size (0.0288 μm^2) is found in the higher the densified (84%) specimen.
- Reduction in pores in the specimen results in the enhancement of thermal conductivity.
- Bigger size grains are observed in the lower density specimen and smaller size grains are observed in the higher density iron specimen due to higher compaction pressure.
- Ferrite grains are observed in the surface morphology of iron specimens.
- The thermal conductivities obtained through regression analysis (DE) modeling and MATLAB software has shown good agreement with the experimental results.
- The software DE and MATLAB could be used for the sintered P/M iron to predict and analyze material's thermal conductivity.
- The ANSYS software could also be used for analyzing the heat flow pattern across the sintered porous iron material.

ACKNOWLEDGMENT

The authors express their sincere gratitude to the Vice Chancellor, SASTRA Deemed to be University, for granting permission to publish their research work. The authors also express their thanks to M/s Hoganas India Ltd, Pune, for their kind gesture in providing iron powder for the present research work.

AUTHORSHIP CONTRIBUTIONS

Authors equally contributed to this work.

DATA AVAILABILITY STATEMENT

The authors confirm that the data that supports the findings of this study are available within the article. Raw data that support the finding of this study are available from the corresponding author, upon reasonable request.

CONFLICT OF INTEREST

The author declared no potential conflicts of interest with respect to the research, authorship, and/or publication of this article.

ETHICS

There are no ethical issues with the publication of this manuscript.

REFERENCE

[1] Vincent C, Silvain JF, Heintz JM, Chandra N. Effect of porosity on thermal conductivity of copper processed by powder metallurgy. J Phys Chem Solids 2012;73:499−504. [CrossRef]

[2] Molina JM, Prieto R, Narciso J, Louis E. The effect of porosity on thermal conductivity of Al-12 wt. % Si/SiC composites. Scr Mater 2009;60:582−585. [CrossRef]

[3] Jiyuan Xu, Yong Zou, Mingxiu Fan, Lin Cheng. Effect of pore parameters on thermal conductivity of sintered LHP wicks. Int J Heat Mass Transf 2012;55:2702−2706. [CrossRef]

[4] Pia G, Sanna U. An intermingled fractal unit's model to evaluate pore size distribution. Appl Therm Engineer 2014;65:330−336. [CrossRef]

[5] Saritas S, Doherty RD, Lawley A. Effect of porosity on the hardenability of P/M steels. Int J Powder Matall 1986;38:31−40.

[6] Daninnger H, Gierl C, Muehlbauer G, Gonzalez MS, Schmidt J, Specht E. Thermal expansion and thermal conductivity of sintered steels- the real effect of porosity. Int J Powder Metall 2011;47:31−41.

[7] Miura S, Terada Y, Suzuki T, Liu CT, Mishima Y. Thermal conductivity of Ni-Al powder compacts for reaction synthesis. Intermetall 2000;8:151−155. [CrossRef]

[8] Gojic M, Suceskka M, Rajic M. Thermal analysis of low alloy Cr-Mo steel. J Therm Anal Calorim 2004;75:947−956. [CrossRef]

[9] Popovska N, Alkhateeb E, Froba AP, Leipertz A. Thermal conductivity of porous Si C composite ceramics derived from paper precursor. Ceram Int 2010;36:2203−2207. [CrossRef]

[10] Biceroglu O, Mujumdar AS, Van Heiningin ARP, Douglas WJM. Thermal conductivity of sintered metal powders at room temperature. J Heat Mass Transf 1976;3:183−192. [CrossRef]

[11] Tatar C, Demir NO. Investigation of thermal conductivity and microstructure of Al_2O_3 particulate reinforced aluminium composites by Powder metallurgy method. Phys B Condens Matter 2010;405:896−899. [CrossRef]

[12] Zivcova Z, Gregorova E, Pabst W, Smith DS, Michot A, Poulier C. Thermal conductivity of porous alumina ceramics prepared using starch as a pore forming agent. J Eur Ceram Soc 2009;29:347−353. [CrossRef]

[13] Kurt A, Ates H. Effect of porosity on thermal conductivity of powder metal materials. Mater Des 2007;28:230−233. [CrossRef]

[14] Matsuo H. The effect of porosity on thermal conductivity of nuclear graphite. J Nucl Mater 1980;89:9−12. [CrossRef]

[15] Ondracek G, Schulz B. The porosity dependence of thermal conductivity for nuclear fuels. J Nucl Mater 1973;46:253−258. [CrossRef]

[16] Bauer S, Urquhart A. Thermal and physical properties of reconsolidated crushed rock salt as a function of porosity and temperature. Acta Geotech 2016;11:913−924. [CrossRef]

[17] Liu XL, Song FZ, Xu Q, Luo QY, Tian Y, Li JW, et al. The influence of pore size distribution on thermal conductivity, permeability, and phase change behavior of hierarchical porous materials. Sci China Tech Sci 2021;64:2485−2494. [CrossRef]

[18] Hossain ME. Role of porosity on energy transport with equal rock-fluid temperatures during thermal EOR process. Arab J Sci Engineer 2017;42:1621−1631. [CrossRef]

[19] Li KQ, Li DQ, Chen DH, Gu SX, Liu Y. A generalized model for effective thermal conductivity of soils considering porosity and mineral composition. Acta Geotech 2021;16:3455−3466. [CrossRef]

[20] Hussain EM. Effect of the porosity on a porous plate saturated with a liquid and subjected to a sudden change in temperature. Acta Mech 2018;229:2431−2444. [CrossRef]

[21] Kandavel TK, Dhasarathy S. Experimental investigation on thermal behaviour of copper-added P/M iron materials at different sintering temperatures. Aust J Mech Engineer 2021;19;57−62. [CrossRef]